Published in final edited form as:
Glia. 2012 September ; 60(9): 1316–1329. doi:10.1002/glia.22351.

Differential distribution of diacylglycerol lipase-alpha and N-acylphosphatidylethanolamine-specific phospholipase D immunoreactivity in the superficial spinal dorsal horn of rats

Zoltán Hegyi[1], **Krisztina Holló**[1], **Gréta Kis**[1], **Ken Mackie**[2], and **Miklós Antal**[1]

[1]Department of Anatomy, Histology and Embryology, Faculty of Medicine, Medical and Health Science Center, University of Debrecen, H-4032 Debrecen, Hungary

[2]Department of Psychological and Brain Sciences, Indiana University, Bloomington, Indiana, USA

Abstract

It is generally accepted that the endocannabinoid system plays important roles in spinal pain processing. Although it is documented that cannabinoid-1 receptors are strongly expressed in the superficial spinal dorsal horn, the cellular distribution of enzymes that can synthesize endocannabinoid ligands is less well studied. Thus, using immunocytochemical methods at the light and electron microscopic levels, we investigated the distribution of diacylglycerol lipase-alpha (DGLα) and N-acylphosphatidylethanolamine-specific phospholipase D (NAPE-PLD), enzymes synthesizing the endocannabinoid ligands, 2-arachidonoylglycerol (2-AG) and anandamide, respectively. Positive labeling was revealed only occasionally in axon terminals, but dendrites displayed strong immunoreactivity for both enzymes. However, the dendritic localization of DGLα and NAPE-PLD showed a remarkably different distribution. DGLα immunolabeling in dentrites was always revealed at membrane compartments in close vicinity to synapses. In contrast to this, dendritic NAPE-PLD labeling was never observed in association with synaptic contacts. In addition to dendrites, a substantial proportion of astrocytic (immunoreactive for GFAP) and microglial (immunoreactive for CD11b) profiles were also immunolabeled for both DGLα and NAPE-PLD. Glial processes immunostained for DGLα were frequently found near to synapses in which the postsynaptic dendrite was immunoreactive for DGLα, whereas NAPE-PLD immunoreactivity on glial profiles at the vicinity of synapses was only occasionally observed. Our results suggest that both neurons and glial cells can synthesize and release 2-AG and anandamide in the superficial spinal dorsal horn. 2-AG can primarily be released by postsynaptic dendrites and glial processes adjacent to synapses, whereas anandamide can predominantly be released from non-synaptic dendritic and glial compartments.

Keywords

DGLα; NAPE-PLD; nociceptive primary afferents; interneurons; glial cells

INTRODUCTION

Cannabinoid receptors (CB_1-Rs) (Matsuda et al., 1990) are the most abundant neuromodulatory receptors in the brain and spinal cord (Herkenham et al., 1991; Matsuda et al., 1993; Tsou et al., 1998), where they are primarily activated by two major endogenous

Corresponding author: Miklós Antal, MD, PhD, DSc, Department of Anatomy, Histology and Embryology, Faculty of Medicine, Medical and Health Science Center, University of Debrecen, Nagyerdei krt 98. 4032 Debrecen, Hungary, Tel: +36 52 255567, Fax: +36 52 255115, antal@anat.med.unideb.hu.

ligands, anandamide and 2-arachidonoylglycerol (2-AG) (Devane et al., 1992; Sugiura et al., 1995; Stella et al., 1997). There is also general agreement that as a conserved feature of many glutamatergic synapses 2-AG is synthetised by diacylglycerol lipase alpha (DGLα) (Bisogno et al., 1997, 1999; Stella et al., 1997) in postsynaptic neurons, from where it is released in an activity-dependent manner. The released 2-AG acts retrogradely on presynaptic CB_1-Rs (Katona et al., 1999, 2006; Kawamura et al., 2006; Katona and Freund, 2008), causing short- and long-term suppression of transmitter release (Kano et al., 2009).

It is important to understand cannabinoid signaling in neural circuits of the superficial spinal dorsal horn. Cannabinoids play major roles in pain processing by suppressing noxious stimulus-evoked activity in spinal nociceptive neurons (Hohmann et al., 1995, 1998; 1999; Pacher et al., 2006; Di Marzo, 2008), thus repressing hyperalgesia and allodynia in animal models of chronic pain (Herzberg et al., 1997; Chapman, 1999; Drew et al., 2000; Kelly and Chapman, 2001; Morisset and Urban, 2001; La Rana et al., 2006). According to the most accepted hypothesis, cannabinoid-evoked spinal pain suppression is mediated by the following mechanisms: release of glutamate from incoming nociceptive primary afferents activates group I metabotropic glutamate receptors (mGluR's), phospholipase-Cβ (PLCβ), and DGLα and thus evokes 2-AG release from postsynaptic neurons (Nyilas et al., 2009). Acting on presynaptic CB_1-Rs (Farquhar-Smith et al., 2000; Nyilas et al., 2009), 2-AG then suppresses the transmission of nociceptive signals from primary afferents to spinal neurons.

Recent findings, however, raised doubts about the validity of this simple model and have created controversies regarding the function and molecular architecture of the spinal endocannabinoid system. Recently, we reported that CB_1-Rs can be demonstrated only on a fraction, 49% and 22% of peptidergic and non-peptidergic nociceptive primary afferents, respectively (Hegyi et al. 2009). Causing further complications, a recent report (Pernia-Andrade et al., 2009) demonstrated that CB_1 receptor activation decreases gamma-aminobutyric acid (GABA) release from inhibitory interneurons in the dorsal horn. The resulting decrease in inhibitory tone means that activating CB_1 receptors might have pronociceptive actions.

It appears that the contribution of endocannabinoid mechanisms to spinal pain processing can not be understood without a more comprehensive knowledge about the molecular architecture of the spinal endocannabinoid signaling machinery. To obtain a comprehensive overview about the organization of the spinal cannabinoid system, we have recently provided a detailed description about the cellular localization of CB_1-Rs in the superficial spinal dorsal horn (Hegyi et al. 2009). Here we investigated the cellular distribution of diacylglycerol lipase-alpha (DGLα) and N-acylphosphatidylethanolamine-specific phospholipase D (NAPE-PLD), enzymes important in the synthesis of the two major endocannabinoids, 2-AG and anandamide.

MATERIALS AND METHODS

Animals and preparation of tissue sections

Experiments were carried out on 9 adult rats (Wistar-Kyoto, 250–300 g, Gödöllő, Hungary), two wild-type and one NAPE-PLD knock-out mice. All animal study protocols were approved by the Animal Care and Protection Committee at the University of Debrecen, and were in accordance with the European Community Council Directives and the rules of the Indiana University Institutional Animal Care and Use Committee. The animals were deeply anesthetized with sodium pentobarbital (50 mg/kg, i.p.) and transcardially perfused with Tyrode's solution (oxygenated with a mixture of 95% O_2, 5% CO_2), followed by a fixative containing either (1) 4% paraformaldehyde (3 adult rats and all mice; for peroxidase based single and fluorescent double immunostaining) or (2) 4% paraformaldehyde and 0.1%

glutaraldehyde (3 adult rats; for preembedding immunostaining for electronmicroscopy) dissolved in 0.1 M phosphate buffer (PB, pH 7.4). After the transcardial fixation, the L3–L5 lumbar segments of the spinal cord were removed, post-fixed in their original fixative for 1–4 hours, and immersed into 10% and 20% sucrose dissolved in 0.1 M PB until they sank. In order to enhance reagent penetration the removed spinal cord was freeze-thawed in liquid nitrogen. Fifty μm thick transverse sections were cut on a vibratome, and the sections extensively washed in 0.1 M PB.

Immunohistochemistry

Single immunostaining—A single immunostaining protocol was performed to study the laminar distribution of DGLα and NAPE-PLD. Free-floating sections were first incubated in rabbit anti-DGLα (1:1000, termed "INT" in Katona et al., 2006) or guinea pig anti-NAPE-PLD antibody (diluted 1:200; catalog no.: NAPE-PLD-GP-Af720, Frontier Science Co., Ishikari, Hokkaido, Japan) for 48 hours at 4 °C, and then were transferred into biotinylated goat anti-rabbit IgG or goat anti-guinea pig IgG (diluted 1:200; catalog no.: PK-4001 and BA-7000, respectively, Vector Labs., Burlingame, California, USA) for 12 hours at 4°C. Thereafter, the sections were treated with an avidin biotinylated horseradish peroxidase complex (diluted 1:100, Vector Labs., Burlingame, California, USA) for 5 hours at room temperature, and the immunoreaction was completed with a 3,3′-diaminobenzidin (catalog no.: D-5637, Sigma, St. Louis, Missouri, USA) chromogen reaction. Before the antibody treatments the sections were kept in 10% normal goat serum (catalog no.: S-1000, Vector Labs., Burlingame, California, USA) for 50 minutes. Antibodies were diluted in 10 mM Tris-phosphate-buffered isotonic saline (TPBS, pH 7.4) to which 1% normal goat serum (catalog no.: S-1000, Vector Labs., Burlingame, California, USA) was added. Sections were mounted on glass slides, dehydrated and covered with Permount neutral medium.

Double immunostaining—Double-immunostaining protocols were performed to study the co-localization of DGLα and NAPE-PLD immunoreactivity with various markers of nociceptive primary afferents, axon terminals of putative glutamatergic and GABAergic spinal neurons, astrocytes and microglial cells. Free-floating sections were first incubated with a mixture of antibodies that contained rabbit anti-DGLα (1:1000, termed "INT" in Katona et al., 2006) or guinea pig anti-NAPE-PLD antibody (diluted 1:200; catalog no.: NAPE-PLD-GP-Af720, Frontier Science Co., Ishikari, Hokkaido, Japan) and one of the following antibodies: (1) guinea pig anti-calcitonin gene-related peptide (CGRP) (diluted 1:2000, catalog no.: T5027, Peninsula Labs, San Carlos, California, USA), (2) rabbit anti-calcitonin gene-related peptide (CGRP) (diluted 1:10.000, catalog no.: 15360, Millipore, Temecula, California, USA) (3) biotinylated isolectin B4 (IB4) (1:2000, catalog no.: I21414, Invitrogen, Eugene, Oregon, USA), (4) guinea pig anti-vesicular glutamate transporter 2 (VGLUT2) (diluted 1:2000, catalog no.: AB2251, Millipore, Temecula California, USA), (5) mouse anti-vesicular glutamate transporter 2 (VGLUT2) (diluted 1:10.000, catalog no.: MAG5504, Millipore, Temecula, California, USA) (6) a mixture of mouse anti-glutamic acid decarboxylase 65 and mouse anti-glutamic acid decarboxylase 67 (GAD65 and GAD67) (diluted 1:1000, catalog no.: MAB351 and MAB5406, Millipore, Temecula, California, USA), (5) mouse anti-glial fibrillary acidic protein (GFAP) (diluted 1:1000, catalog no.: MAB3402, Millipore, Temecula, California, USA), and (6) mouse anti-CD11b (diluted 1:500, catalog no.: MCA275G, AbD Serotec, Oxford, UK). The sections were incubated in the primary antibody solutions for 2 days at 4 °C and were transferred for an overnight treatment into the appropriate mixtures of secondary antibodies that were selected from the following: goat anti-rabbit IgG conjugated with Alexa Fluor 555 (diluted 1:1000, catalog no.: A21428, Invitrogen, Eugene, Oregon, USA), goat anti-guinea pig IgG conjugated with Alexa Fluor 488 (diluted 1:1000, catalog no.: A11073, Invitrogen, Eugene, Oregon, USA), goat anti-mouse IgG conjugated with Alexa Fluor 488 (diluted 1:1000,

catalog no.: A11001, Invitrogen, Eugene, Oregon, USA), goat anti-guinea pig IgG conjugated with Alexa Flour 555 (diluted 1:1000, catalog no.: A21435, Invitrogen, Eugene, Oregon, USA), goat anti-rabbit IgG conjugated with Alexa Flour 488 (diluted 1:1000, catalog no.: A11034, Invitrogen, Eugene, Oregon, USA) and streptavidin conjugated with Alexa Fluor 488 (diluted 1:1000, catalog no.: S11223, Invitrogen, Eugene, Oregon, USA). Before the antibody treatments the sections were kept in 10% normal goat serum (catalog no.: S-1000, Vector Labs., Burlingame, California, USA) for 50 minutes. Antibodies were diluted in 10 mM TPBS (pH 7.4) to which 1% normal goat serum (catalog no.: S-1000, Vector Labs., Burlingame, California, USA) was added. Sections were mounted on glass slides and covered with Vectashield (catalog no.: H-1000, Vector Labs, Burlingame, California, USA).

Confocal microscopy and analysis—Series of 1 μm thick optical sections with 0.3 μm separation in the Z axis were scanned with an Olympus FV1000 confocal microscope. Scanning was carried out using a 60x oil-immersion lens (NA: 1.4). The confocal settings (laser power, confocal aperture and gain) were identical for all sections, and care was taken to ensure that no pixels corresponding to immunostained puncta were saturated. The scanned images were processed by Adobe Photoshop CS5 software.

The co-localization of DGLα and NAPE-PLD with the investigated markers was quantitatively analyzed in the double-stained sections. A 10 × 10 standard square grid in which the edge-length of the unit square was 4 μm (the whole grid was 40 μm × 40 μm in size) was placed onto the regions of confocal images corresponding to laminae I–II of the superficial spinal dorsal horn. The proper placement of the grid was based on the following criteria: a) The border between the dorsal column and the dorsal horn was easily identified on the basis of the intensity of immunostaining. b) The border between laminae II and III was approximated on the basis of previous ultrastructural observations (McClung and Castro, 1978; Molander et al., 1984; McNeill et al., 1988). Thus, immunoreactivities and co-localizations were investigated in the most superficial 150 μm thick zone of the dorsal horn that had earlier been identified as a layer of the gray matter corresponding to laminae I and II in the L3-L5 segments of the spinal dorsal horn.

Profiles that showed immunoreactivity for DGLα or NAPE-PLD over the edges of the standard grid were counted in the medial and lateral compartments of laminae I and II. The selected profiles were then examined whether they were also immunoreactive for the axonal or glial markers. Since the DGLα and NAPE-PLD antibodies utilized in the present study were raised against the intracellular domain of the enzyme, to define the co-localization values we counted only those DGLα or NAPE-PLD immunolabeled puncta that were located within the confines of the areas immunostained for the marker. The co-localization for all investigated markers was analyzed in three animals. The quantitative measurement was carried out in three sections that were randomly selected from each animal. Thus the calculation of quantitative figures, mean values and standard error of means (SEM), was based on the investigation of nine sections.

Preembedding immunostaining with diaminobenzidine chromogen reaction for electronmicroscopy—A preembedding immunostaining similar to the single immunostaining protocol described above was performed to study the cellular distribution of DGLα and NAPE-PLD at the ultrastructural level. Following extensive washes in 0.1 M PB (pH 7.4) and a treatment with 1% sodium borohydride for 30 minutes, free-floating sections from animals fixed with 4% paraformaldehyde and 0.1% glutaraldehyde were first incubated with rabbit anti-DGLα (1:1000, termed “INT” in Katona et al., 2006) or guinea pig anti-NAPE-PLD antibody (diluted 1:200; catalog no.: NAPE-PLD-GP-Af720, Frontier Institute Co., Ishikari, Hokkaido, Japan) for 48 hours at 4 °C, than were transferred into biotinylated

goat anti-rabbit IgG or goat anti-guinea pig IgG (diluted 1:200; catalog no.: PK-4001 and BA-7000, respectively, Vector Labs., Burlingame, California, USA) for 12 hours at 4°C. Thereafter, the sections were treated with an avidin biotinylated horseradish peroxidase complex (diluted 1:100, catalog no.: PK-4001, Vector Labs., Burlingame, California, USA) for 5 hours at room temperature, and the immunoreaction was completed with a 3,3′-diaminobenzidine (catalog no.: D-5637, Sigma, St. Louis, Missouri, USA) chromogen reaction. Before the antibody treatments the sections were kept in 10% normal goat serum (catalog no.: S-1000, Vector Labs., Burlingame, California, USA) for 50 minutes. Antibodies were diluted in 10 mM Tris-phosphate-buffered isotonic saline (TPBS, pH 7.4). Immunostained sections were treated with 0.5% osmium tetroxide for 45 minutes, then dehydrated and flat-embedded into Durcupan ACM resin (catalog no.: 44610, Sigma, St. Louis, Missouri, USA) on glass slides. Selected sections were re-embedded, ultrathin sections were cut and collected on Formvar-coated single-slot nickel grids, and counterstained with uranyl acetate and lead citrate.

Preembedding nanogold immunostaining for electron microscopy—A preembedding nanogold immunohistochemical protocol was performed to study the cellular distribution of DGLα and NAPE-PLD with high resolution. Following extensive washes in 0.1 M PB (pH 7.4) and treatment with 1% sodium borohydride for 30 minutes, free-floating sections from animals fixed with 4% paraformaldehyde and 0.1% glutaraldehyde were first incubated in rabbit anti-DGLα (1:1000, termed “INT” in Katona et al., 2006) or guinea pig anti-NAPE-PLD antibody (diluted 1:200; catalog no.: NAPE-PLD-GP-Af720, Frontier Institute Co., Ishikari, Hokkaido, Japan) for 48 hours at 4 °C. The sections were then transferred into a solution of goat anti-rabbit or goat anti guinea pig IgG conjugated to 1 nm gold particles (1:100, Aurion, Wageningen, The Netherlands) for 12 hours at 4 °C. After repeated washing in 0.01 M Tris-buffered isotonic saline (TBS, pH 7.4), the sections were post-fixed for 10 minutes in 2.5% glutaraldehyde and washed again in 0.01 M TBS and 0.1 M PB. The gold labeling was intensified with a silver enhancement reagent (Aurion R-GENT, Wageningen, The Netherlands). Sections were treated with 1% osmium tetroxide for 45 minutes, then dehydrated and flat-embedded into Durcupan ACM resin (Sigma, St. Louis, Missouri, USA) on glass slides. Selected sections were re-embedded, ultrathin sections were cut and collected on Formvar-coated single-slot nickel grids, and counterstained with uranyl acetate and lead citrate.

RESULTS

Distribution of DGLα and NAPE-PLD immunoreactivity in the superficial spinal dorsal horn

To elucidate the distribution of the DGLα protein in laminae I–II of the spinal dorsal horn, immunostaining for DGLα with an antibody directed against a long internal segment of the enzyme (residues 790–908) (Katona et al., 2006) was carried out in the rat lumbar spinal cord. Both peroxidase-based and fluorescence single immunostaining revealed an abundant immunoreactivity for DGLα throughout the superficial spinal dorsal horn. Lamina II appeared as a heavily stained band on the cross-section of the spinal cord, whereas lamina I and the deeper laminae of the dorsal horn were more sparsely stained (Fig. 1a, b). Immunostained elements appeared as punctate profiles both in the densely and sparsely stained zones (Fig. 1a, b). Besides the characteristic punctate labeling, larger immunoreactive spots resembling somata of neurons or glial cells were also scattered both in the gray and white matters (Fig. 1a, b).

To reveal immunonoreactivity for NAPE-PLD, sections of the lumbar spinal cord were reacted with a highly specific anti-NAPE-PLD antibody raised against the N-terminal 41 aa of the enzyme (Nyilas et al., 2008). Here, we observed a punctate immunostaining for

NAPE-PLD, the density of which was more or less homogeneous throughout the entire cross-sectional area of the dorsal horn including laminae I and II (Fig. 1c, d). Similarly to DGLα, larger NAPE-PLD immunoreactive spots resembling somata of neurons or glial cells were also observed (Fig. 1c, d).

Co-localization of DGLα and NAPE-PLD immunoreactivity with markers of nociceptive primary afferents

C and Aδ type primary afferents terminate almost exclusively in lamiae I–II of the spinal dorsal horn and transmit mostly nociceptive signals from peripheral receptors to the spinal cord (Ribeiro da Silva and De Korninck, 2009). Synaptic transmission from a population of these nociceptive primary afferents to spinal neurons is mediated only by glutamate, whereas others also release neuropeptides in addition to glutamate (Willis and Coggeshall, 2004). Most of the peptidergic nociceptive primary afferents express calcitonin gene-related peptide (CGRP), whereas the cell membrane of the non-peptidergic axon terminals contains a polysaccharide that selectively binds the lectin isolated from *Bandeiraea simplicifolia*, isolectin-B4 (IB4) (Willis and Coggeshall, 2004; Ribeiro da Silva and De Korninck, 2009). Thus, to study the expression of DGLα and NAPE-PLD on central axon terminals of peptidergic and non-peptidergic nociceptive primary afferents we investigated the co-localization of the enzymes with CGRP immunoreactivity and IB4-binding.

In agreement with previous studies, we observed a strong immunostaining for CGRP in laminae I-IIo (Traub et al., 1989; Nasu, 1999) (Supporting Information Figure 5a, b). Investigating the co-localization between DGLα and CGRP immunoreactivity, we collected 703 and 1224 profiles immunostained for CGRP and DGLα, respectively, and found that only 1.96 ± 0.78 % of DGLα immunoreactive puncta were also stained for CGRP, whereas 3.41 ± 1.11 % of CGRP immunoreactive axon terminals proved to be immunoreactive also for DGLα in laminae I–II of the dorsal horn (Figs. 2a, 3). The co-localization values for NAPE-PLD were even lower. Following a careful analysis of 760 and 1304 profiles immunostained for CGRP and NAPE-PLD, respectively, we found that 1.69 ± 0.91 % of NAPE-PLD immunoreactive puncta were also stained for CGRP, whereas 1.97 ± 0.76 % of CGRP immunoreactive axon terminals proved to be immunoreactive also for NAPE-PLD in the superficial spinal dorsal horn (Figs. 2a, 3).

As it has been reported earlier, IB4-binding labeled a large number of axon terminals in lamina IIi (Guo et al., 1999) (Supporting Information Figure 5c, d). In contrast to some earlier reports demonstrating IB4-binding to astrocytes and microglial cells (Streit, 1990; Villeda et al., 2006; Runyan et al., 2007), we have never seen IB4-binding on glial cells in the present study (Supporting Information Figure 6). Despite the strong immunostaining and the substantial spatial overlap between the investigated profiles, the co-localization between axon terminals labeled with IB4-binding and puncta immunoreactive for DGLα or NAPE-PLD was very low. After the investigation of 660 IB4-binding and 1490 DGLα immunostained profiles, it was found that 2.48 ± 0.99 % of DGLα immunoreactive puncta were also positive for IB4-binding, whereas 1.06 ± 0.79 % of axon terminals that were positive for IB4-binding proved to be immunoreactive also for DGLα (Figs. 2c, 3). The co-localization values for NAPE-PLD were very similar. From 737 IB4-binding and 1355 DGLα immunostained profiles 1.92 ± 0.88 % of NAPE-PLD immunoreactive puncta were also positive for IB4-binding, and 2.43 ± 0.91 of axon terminals that were positive for IB4-binding proved to be immunoreactive also for NAPE-PLD in the superficial spinal dorsal horn (Figs. 2d, 3).

Co-localization of DGLα and NAPE-PLD immunoreactivity with markers of axon terminals of putative glutamatergic and GABAergic spinal neurons

There is general agreement that VGLUT2 can be used as a marker for axon terminals of intrinsic spinal neurons (Li et al., 2003; Oliveira et al., 2003; Todd et al, 2003). It is also well accepted that GABAergic neurons synthesize GABA with the aid of glutamic acid decarboxylase (GAD) (Martin et al., 2000). All GABAergic neurons in the spinal cord are thought to contain both isoforms of GAD (GAD65 and GAD67) (Mackie et al., 2003; Tran et al., 2003), although the relative amounts of the two enzymes vary widely among different cell populations (Soghomonian and Martin, 1988; Mackie et al., 2003). Therefore, to study the expression of DGLα and NAPE-PLD on central axon terminals of putative glutamatergic and GABAergic spinal neurons we investigated co-localization between the enzymes and VGLUT2 as well as GAD65/67 immunoreactivities.

Confirming results of previous studies (Li et al., 2003; Oliviera et al., 2003; Todd et al, 2003), VGLUT2 immunoreactive axon terminals were homogeneously distributed in laminae I–II (Supporting Information Figure 5e, f). The co-localization values between the investigated enzymes and VGLUT2 immunoreactivity were slightly higher than were found for the co-localization with axon terminals of nociceptive primary afferents, but were still very low. Evaluating 725 and 1508 profiles immunostained for VGLUT2 and DGLα, respectively, we found that 3.78 ± 0.59 % of DGLα immunoreactive puncta were also immunostained for VGLUT2, whereas 6.76 ± 0.47 % of axon terminals that were positive for VGLUT2 were also immunoreactive for DGLα (Figs. 2e, 3). The co-localization values for NAPE-PLD were even lower. In this case, after the investigation of 681 and 1526 profiles immunostained for VGLUT2 and NAPE-PLD, respectively, it was revealed that 2.23 ± 1.67 % of NAPE-PLD immunoreactive puncta were also stained for VGLUT2, whereas 3.96 ± 1.31 of VGLUT2 immunoreactive axon terminals proved to be immunoreactive also for NAPE-PLD (Figs. 2f, 3).

Similar to earlier reports (Feldblum et al., 1995; Mackie et al., 2003), GAD65/67 immunoreactive axon terminals showed a dense distribution in the superficial spinal dorsal horn (Supporting Information Figure 5g, h). Investigating the co-localization between DGLα and GAD 65/67 immunoreactivity, we collected 641 and 1388 profiles immunstained for GAD65/67 and DGLα, respectively, and found that 2.16 ± 043 % of DGLα immunoreactive puncta were also stained for GAD65/67, whereas 3.12 ± 0.93 % of GAD65/67 immunoreactive axon terminals proved to be immunoreactive also for DGLα (Figs. 2g, 3). The co-localization values for NAPE-PLD were approximately similar. From 707 and 1431 puncta immunostained for GAD65/67 and NAPE-PLD, respectively, 0.91 ± 0.7 % of NAPE-PLD immunoreactive puncta were also positive for GAD65/67, and 2.11 ± 1.06 % of axon terminals that were immunostained for GAD65/67 turned out also to be immunoreactive for NAPE-PLD in laminae I–II (Figs. 2h, 3)

Co-localization of DGLα and NAPE-PLD immunoreactivity with markers of astrocytes and microglial cells

A great deal of experimental evidence has accumulated in recent years suggesting the existence of a bidirectional communication between glial cells and neurons (Araque et al., 2001; Volterra and Bezzi, 2002; Nedergaard et al., 2003; Haydon and Carmingnoto, 2006; Suter et al., 2007; Zhang et al., 2008). It has also been demonstrated that CB_1-Rs are expressed by astrocytes and microglial cells in various parts of the central nervous system including the spinal dorsal horn (Rodriquez et al., 2001; Salio et al., 2002; Cabral and Marciano-Cabral, 2005; Navarrate and Araque, 2008; Hegyi et al., 2009). Production and inactivation of endocannabinoids, anandamide and 2-AG, by cultured astrocytes and microglial cells have also been shown in many studies (Walter et al., 2002, 2003, 2004;

Marsicano et al. 2003; Walter and Stella, 2003, 2004; Carrier et al., 2004). Thus, because of their potential importance in spinal pain processing we investigated the localization of DGLα and NAPE-PLD on astrocytes and microglial cells by using glial fibrillary acidic protein (GFAP) and CD11b as markers for astrocytes and microglial cells, respectively.

We observed strong immunolabeling in the superficial spinal dorsal horn for both glial markers that was identical to that reported earlier (Garrison et al., 1991; Eriksson et al., 1993; Molander et al., 1997) (Supporting Information Figure 5i–l). Investigating the co-localization between DGLα and GFAP immunoreactivity, we collected 216 and 1321 profiles immunoreactive for GFAP and DGLα, respectively, and found that 9.39 ± 1.96 % of DGLα immunoreactive puncta also stained for GFAP, whereas 33.33 ± 2.06 % of GFAP immunoreactive profiles proved to be immunoreactive also for DGLα (Figs. 3, 4a–c). In addition to GFAP, we revealed a substantial co-localization between DGLα and CD11b immunoreactivity. Moreover, DGLα showed a much stronger co-localization with CD11b immunoreactive profiles than with structures stained for GFAP. For the microglial marker, after the investigation of 207 and 1297 profiles immunstained for CD11b and DGLα, respectively, the co-localization analysis showed that 29.53 ± 1.19 % of DGLα immunoreactive puncta were also stained for CD11b, whereas 67.15 ± 2.21 % of CD11b immunoreactive profiles were also immunoreactive for DGLα (Figs. 3, 4d–f).

The co-localization values between NAPE-PLD and the glial markers were very similar to the figures that we obtained for the co-localization between DGLα and the same glial markers. However, there was a tendency for NAPE-PLD to have a slightly higher expression on glial cells than DGLα. We collected 241 and 1406 profiles immunoreactive for GFAP and NAPE-PLD, respectively, and found that 12.52 ± 2.15 % of NAPE-PLD immunoreactive puncta were also stained for GFAP, whereas 54.77 ± 1.98 % of GFAP immunoreactive profiles were also immunoreactive for NAPE-PLD in the superficial spinal dorsal horn (Figs. 3, 4g–i). In addition, we investigated 223 and 1501 profiles immunoreactive for CD11b and NAPE-PLD, respectively, and observed that 32.11 ± 2.30 % of NAPE-PLD immunoreactive puncta were also stained for CD11b, whereas 75.34 ± 2.60 % of CD11b immunoreactive profiles were immunoreactive for NAPE-PLD (Figs. 3, 4j–l).

In order to substantiate the glial localization of the enzymes, in addition to the X-Y dimensions the confocal optical sections were also investigated in the X-Z and Y-Z projections. The X-Z and Y-Z images were drawn through the point of co-localization between the two markers, and the two orthogonal views were investigated for overlap. An example of this type of investigation is demonstrated on Figure 5, where the X-Z and Y-Z projections of confocal images shown in Figure 4i are illustrated.

Ultrastructural localization of DGLα and NAPE-PLD immunoreactivity

Ultrathin sections immunostained for DGLα and NAPE-PLD were investigated at the ultrastructural level. After finding a minimal overlap between immunolabeling for DGLα and NAPE-PLD with various axonal markers and an extensive co-localization between DGLα, and NAPE-PLD with markers for astrocytes and microglial cells in double immunostained sections, we defined the sub-cellular localization of DGLα and NAPE-PLD both in axon terminals and glial profiles. Furthermore, since we recovered only approximately half of the DGLα and NAPE-PLD immunoreactive puncta on axon terminals and glial cells in the co-localization studies, an extensive search for DGLα and NAPE-PLD immunolabeling in the somato-dendritic compartment of neurons was also carried out.

In agreement with the results obtained from the co-localization studies, peroxidase reaction precipitates and silver intensified nanogold particles labeling DGLα and NAPE-PLD were recovered primarily in dendrites (Figs. 6a–c, f–h, 7a, b, d) and glial processes (Figs. 6a, b, e,

7e, f), and were found only occasionally in axon terminals (Figs. 6d, 7c). Regardless of whether the labeled profile was a dendrite, glia-like process or an axon terminal, immunolabeling was revealed exclusively in close association to the plasma membrane (Figs.6, 7). The membrane-associated immunoprecipitates and nanogold particles were found at the cytoplasmic face of the plasma membrane (Figs. 6–7), in agreement with the intracellular location of the epitopes recognized by the antibodies.

In dendrites, the end product of the immunoperoxidase and nanogold staining for DGLα was observed at membrane compartments where the dendrites received synaptic contacts from axon terminals with different morphology (Fig. 6a–c, f–h), including boutons representing the central element of synaptic glomeruli (Fig. 6c). Regardless of the morphology of the presynaptic axon, immunolabeling for DGLα was always observed adjacent or in close vicinity to synaptic apposition. In case of the nanogold staining, silver intensified gold particles were found in perisynaptic position at asymmetric synaptic contacts (Figure 6f–h). In the case of the immunoperoxidase staining, the immunoprecipitate also covered a part of the postsynaptic membrane (Figure 6a, b). Similar to DGLα, immunolabeling for NAPE-PLD in dendrites also appeared as small immunoprecipitates associated with the inner surface of the cell membrane (Fig. 7a, b, d). However, these immunolabeled membrane compartments were never observed in close vicinity to synaptic appositions (Fig. 7a, b, d), although this finding may be limited by the fact that we investigated single and not serial ultrathin sections.

In axon terminals, labeling was only occasionally found for either DGLα or NAPE-PLD (Figs. 6d, 7c). In some cases the labeled membrane segments were adjacent to synaptic contacts (Fig. 6d), in other cases there was no sign of synaptic specialization in the vicinity of the labeled membrane compartments (Fig. 7c). We have to add, however, that we studied single and not serial ultrathin sections, thus the accurate relationship between the sites of labeling and synapses formed by the labeled axon terminal can not be definitively determined from our observations.

In glia-like processes, the labeling was abundant for both DGLα (Fig. 6a, b, d) and NAPE-PLD (Fig. 7e, f). Immunolabeled glia-like processes were frequently observed. It was a general finding that the membrane compartment immunureactive for DGLα or NAPE-PLD was restricted only to a segment of the glial membrane, while the adjacent part of the glial profile was free of labeling (Figs. 7b, e, 7e, f). In the case of DGLα, immunostained glia-like processes were frequently revealed in close vicinity to synaptic contacts between axon terminals and postsynaptic dendrites immunoreactive for DGLα (Fig. 6a, b). In case of NAPE-PLD, however, dendritic segments immunoreactive for the enzyme were never observed in the vicinity of immunoreactive compartments of glial-like processes. Nevertheless, glia-like profiles immunostained for NAPE-PLD were sometimes revealed near to synapses (Fig. 7e). Unfortunately we were not able to define whether the detected immunoprecipitates were in astrocytes or microglial cells, since we can not make any distinction between the profiles of these glial cells in the electronmicroscope.

DISCUSSION

Here we investigated the distribution of DGLα and NAPE-PLD, enzymes involved in synthesizing the endocannabinoid ligands 2-AG and anandamide, respectively, in the superficial spinal dorsal horn of rats. Postsynaptic dendrites displayed strong immunolabeling for both enzymes, but positive staining was revealed only occasionally in axon terminals. Immunolabeling for DGLα in dendrites was always revealed at membrane compartments adjacent to synapses. Dendritic membrane segments immunolabeled for NAPE-PLD, however, were never found to be associated with synapses. In addition to

dendritic expression, both enzymes showed a remarkably strong expression on astrocytes and microglial cells.

Enzymes synthesizing 2-AG and anandamide in the brain and spinal cord

The last step of the major pathway for 2-AG biosynthesis in the brain and spinal cord is catalyzed by diacylglycerol lipase (DGL), which is present in two isoforms in neurons, DGLα and DGLβ (Mechoulam et al., 1995; Sugiura et al., 1995; Bisogno et al., 1997, 1999; Stella et al., 1997; Bisogno et al., 2003). To clarify the relative contribution of DGLα and DGLβ in 2-AG biosynthesis, mutant mouse lines lacking either of the two DGL isoforms were generated (Gao et al., 2010; Tanimura et al. 2010). By analyzing these knockout mice, it was found that endocannabinoid-mediated retrograde synaptic suppression was absent in DGLα knockout mice, whereas it was intact in DGLβ knockout brains. Furthermore, basal 2-AG content was markedly reduced and stimulus-induced elevation of 2-AG was absent in DGLα knockout brains, whereas the 2-AG content was normal in DGLβ knockout animals, indicating that the major enzyme for 2-AG biosynthesis in the adult nervous system is DGLα (Gao et al., 2010; Tanimura et al., 2010).

Anandamide, together with other N-acylethanolamines (NAEs) is synthesized via hydrolysis of the phospholipid precursor N-acylphosphatidylethanolamine (NAPE) (Di Marzo et al., 1994; Schmid et al., 2002; Sugiura et al., 2002). Earlier reports indicated that the conversion of NAPEs to NAEs including anadamide is principally mediated by NAPE-PLD (Sugiura et al., 1996; Okamoto et al., 2004; Morishita et al., 2005; Wang et al., 2006) but analysis of NAPE-PLD-deficient mice and other recent studies revealed the presence of NAPE-PLD independent pathways for the anandamide formation (Leung et al., 2006; Okamoto et al., 2007; Egertova et al., 2008; Liu et al., 2008; Simon and Cravatt, 2008; Wang and Ueda, 2009). While it is important to note that NAPE-PLD is not the only source for anadamide in the brain (Leung et al., 2006; Simon and Cravatt, 2006; Liu et al., 2006), there is still general agreement that NAPE-PLD is a key enzyme capable of generating anandamide from NAPE.

DGLα and NAPE PLD in axon terminals

We found only occasional immunolabeling for DGLα in axon terminals of multiple origins in the superficial spinal dorsal horn. This observation is in good agreement with the results of recent morphological studies confirming that DGLα is primarily localized in postsynaptic dendrites that face CB_1-R expressing terminals (Yoshida et al., 2006; Katona et al., 2006; Suarez et al., 2008; Nyilas et al., 2009).

Our present findings concerning the scanty appearance of NAPE-PLD in axon terminals, however, do not harmonize so well with earlier reports. Authors of some recent articles noted that in higher brain centers NAPE-PLD is concentrated presynaptically in several types of excitatory axon terminals, where it is localized predominantly on the intracellular membrane cisternae of axonal calcium stores (Okamoto et al., 2007; Egertova et al., 2008; Nyilas et al., 2008). The expression of NAPE-PLD in the cell bodies of primary sensory neurons within dorsal root ganglia (DRG) has also been reported (van der Stelt et al., 2005; Nagy et al., 2009). In contrast to this, we observed unexpectedly low levels of NAPE-PLD immunolabeling in axon terminals in the superficial spinal dorsal horn. This finding suggests that the CB_1-R protein is transported from the perikarya of DRG and spinal neurons to their spinal axon terminals in such a limited amount that it is below the threshold of immunocytochemical detection, indicating that the synthesis of anandamide (or other acyl amines) in axon terminals of the dorsal horn by NAPE-PLD may not be very prominent.

Differential distribution of DGLα and NAPE PLD in dendrites

There is general agreement in the literature that 2-AG is released from postsynaptic neurons in an activity dependent manner, travels retrogradely through the synaptic cleft, engages presynaptic CB_1-Rs, which then suppress neurotransmitter release from glutamatergic axon terminals (Kreitzer and Regehr, 2001; Ohno-Shosaku et al., 2001; Maejima et al., 2001; Piomelli, 2003). Variations in this basic scheme accounts for numerous forms of short- and long-term synaptic plasticity and experience-dependent modifications of neuronal activity in the central nervous system (Wilson and Nicoll, 2001, 2002; Chevaleyre et al., 2006; Yoshida et al., 2006; Marinelli et al., 2008). Our present results concerning the perisynaptic dendritic distribution of DGLα are fully consistent with these previous findings.

In contrast to the well established distribution and functional properties of 2-AG-mediated retrograde signaling, the molecular architecture underlying the synthetic side of the anandamide-related endocannabinoid system remains largely unknown, although endogenous anandamide has often been implicated in various behaviors, such as emotion, learning or pain (for review see Kano et al., 2009). In addition, even the sparsely available data addressing the organization of anandamide-related molecular machineries are controversial. As mentioned earlier, most authors have found that NAPE-PLD is concentrated presynaptically in several types of excitatory axon terminals (Okamoto et al., 2007; Egertova et al., 2008; Nyilas et al., 2008). Others, however, argue in favor of a somatodendritic localization of NAPE-PLD (Cristino et al., 2008). Our present findings clearly support the idea of dendritic localization of NAPE-PLD in the superficial spinal dorsal horn.

DGLα and NAPE PLD in glial cells

The expression of functional CB_1-Rs by astrocytes and microglial cells has been reported (Rodriguez et al., 2001; Salio et al., 2002; Walter et al., 2002, 2003, 2004; Walter and Stella, 2003; Navarrete and Araque, 2008; Hegyi et al., 2009). It has also been demonstrated that astrocytes and microglial cells have the potential to produce 2-AG and anandamide and thus can communicate with neighboring neurons through endocannabinoid signaling (Stella and Piomelli, 2001; Ahluwalia et al., 2003; Walter et al., 2002, 2003; Marsicano et al., 2003, Walter and Stella, 2003; Carrier et al., 2004). Endocannabinoid mediated astrocyte-neuron as well as microglial cell-neuron signaling has indeed been reported (Cabral and Marciano-Cabral, 2005; Navarrete and Araque, 2008). Our present results demonstrating an abundant expression of DGLα and NAPE-PLD in both astrocytes and microglial cells provide further evidence for possible communication pathways between glial cells and neurons, as well as between glial cells (Araque et al., 2001; Nedergaard et al., 2003; Haydon and Camignoto, 2006) in the spinal dorsal horn.

The primary activation of the glial endocannabinoid apparatus may arise from neurons (Navarrate and Araque, 2008). In the superficial spinal dorsal horn, the primary activation of neurons in laminae I–II arises from nociceptive primary afferents. From our present results, one may assume that spinal neurons activated by glutamatergic nociceptive primary afferent inputs may release 2-AG from perisynaptic and anandamide from extrasynaptic membrane compartments. The endocannabinoids may diffuse out from their site of release and activate CB_1-Rs on astrocytes and microglial cells (Walter et al., 2002, 2003, 2004; Walter and Stella, 2003; Navarrete and Araque, 2008). CB_1-R activation may lead to phospholipase C-dependent Ca^{2+} mobilization from cytoplasmic stores (Beltramo and Piomelli, 2000; Stella and Piomelli, 2001; Dinh et al., 2002; Witting et al., 2004; Navarrete and Araque, 2008). The increased Ca^{2+} level may activate DGLα and NAPE-PLD resulting in the release of 2-AG and anandamide from glial cells. The released endocannabinoids may diffuse out and, together with 2-AG and anandamide released by dendrites, may act on neural CB_1-Rs

affecting functional properties of spinal neurons remote from their site of release (Bisogno et al., 1999). Alternatively, Gq/11-linked GPCRs expressed on astrocytes and microglia may drive glial endocannabinoid production. Although the way how the glial endocannabinoid system contributes to nociceptive functions remains to be elucidated, the fact that astrocytes and microglial cells express functional CB_1-Rs, DGLα and NAPE-PLD must be considered in the interpretation of effects of cannabinoids on spinal pain processing; especially in chronic pain when the number and activity of microglial cells and asctrocytes are substantially enhanced (Scholz and Woolf, 2007; Cao and Zhang, 2008; Graeber, 2010)

Supplementary Material

Refer to Web version on PubMed Central for supplementary material.

Acknowledgments

This work was supported by the Hungarian National Scientific Research Fund (OTKA 461219), the Hungarian Academy of Sciences (MTA-TKI 242), the US NIH (DA011322 and DA021696) and the TAMOP 4.2.1-08/1-2008-003 project. We thank Serge Luquet for the contributing the colony founder for the NAPE-PLD knockout mice. The project is implemented through the New Hungary Development Plan, co-financed by the European Social Fund and the European Regional Development Fund.

References

Ahluwalia J, Urban L, Bevan S, Nagy I. Anandamide regulates neuropeptide release from capsaicin-sensitive primary sensory neurons by activating both the cannabinoid 1 receptor and the vanilloid receptor 1 in vitro. Eur J Neurosci. 2003; 17:2611–2618. [PubMed: 12823468]

Araque A, Carmignoto G, Haydon PG. Dynamic signaling between neurons and glia. Annu Rev Physiol. 2001; 63:795–813. [PubMed: 11181976]

Beltramo M, Piomelli D. Carrier-mediated transport and enzymatic hydrolysis of the endogenous cannabinoid 2-arachidonylglycerol. Neuroreport. 2000; 11:1231–1235. [PubMed: 10817598]

Bisogno T, Howell F, Williams G, Minassi A, Cascio MG, Ligresti A, Matias I, Schiano-Moriello A, Paul P, Williams EJ, Gagadharan U, Hobbs C, Di Marzo V, Doherty P. Cloning of the first sn1-DAG lipases points to the spatial and temporal regulation of endocannabinoid signaling in the brain. J Cell Biol. 2003; 163:463–468. [PubMed: 14610053]

Bisogno T, Melck D, De Petrocellis L, Di Marzo V. Phosphatidic acid as the biosynthetic precursor of the endocannabinoid 2-arachidonoylglycerol in intact mouse neuroblastoma cells stimulated with ionomycin. J Neurochem. 1999; 72:2113–2119. [PubMed: 10217292]

Bisogno T, Sepe N, Melck D, Maurelli S, De Petrocellis L, Di Marzo V. Biosynthesis, release and degradation of the novel endogenous cannabimimetic metabolite 2-arachidonoylglycerol in mouse neuroblastoma cells. Biochem J. 1997; 322:671–677. [PubMed: 9065792]

Cabral GA, Marciano-Cabral F. Cannabinoid receptors in microglia of the central nervous system: immune functional relevance. J Leukoc Biol. 2005; 78:1192–1197. [PubMed: 16204639]

Cao H, Zhang YQ. Spinal glia activation contributes to pathological pain states. Neurosci Behav Rev. 2008; 32:972–983.

Carrier EJ, Kearn CS, Barkmeier AJ, Breese NM, Yang W, Nithipatikom K, Pfister SL, Campbell WB, Hillard CJ. Cultured rat microglial cells synthesize the endocannabinoid 2-arachidonylglycerol, which increases proliferation via a CB_2 receptor-dependent mechanism. Mol Pharmacol. 2004; 65:999–1007. [PubMed: 15044630]

Chapman V. The cannabinoid CB1 receptor antagonist, SR141716A, selectively facilitates nociceptive responses of dorsal horn neurons in the rat. Br J Pharmacol. 1999; 127:1765–1767. [PubMed: 10482905]

Chevaleyre V, Takahashi KA, Castillo PE. Endocannabinoid-mediated synaptic plasticity in the CNS. Ann Rev Neurosci. 2006; 29:37–76. [PubMed: 16776579]

Cristino L, Starowicz K, De Petrocellis L, Morishita J, Ueda N, Guglielmotti V, Di Marzo V. immunohistochemical localization of anabolic and catabolic enzymes for anadamide and other

putative endovanilloids in the hippocampus and cerebellar cortex of the mouse brain. Neuroscience. 2008; 151:955–968. [PubMed: 18248904]

Devane WA, Hanus L, Breuer A, Pertwee RG, Stevenson LA, Griffin G, Gibson D, Mandelbaum A, Etinger A, Mechoulam R. Isolation and structure of a brain constituent that binds to the cannabinoid receptor. Science. 1992; 258:1946–1949. [PubMed: 1470919]

Di Marzo V. Targeting the endocannabinoid system: to enhance or reduce? Nat Rev Drug Discov. 2008; 7:438–55. [PubMed: 18446159]

Di Marzo V, Fontana A, Cadas H, Schinelli S, Cimino G, Schwartz JC, Piomelli D. Formation and inactivation of endogenous cannabinoid anandamide in central neurons. Nature. 1994; 372:689–691.

Dinh TP, Carpenter D, Leslie FM, Freund TF, Katona I, Sensi SL, Kathuria S, Piomelli D. Brain monoglyceride lipase participating in endocannabinoid inactivation. Proc Natl Acad Sci USA. 2002; 99:10819–10824. [PubMed: 12136125]

Drew LJ, Harris J, Millns PJ, Kendall DA, Chapman V. Activation of spinal cannabinoid 1 receptors inhibits C-fibre driven hyperexcitable neuronal responses and increases [35S]GTPgammaS binding in the dorsal horn of the spinal cord of noninflamed rats. Eur J Neurosci. 2000; 12:2079–2086. [PubMed: 10886347]

Egertova M, Simon GM, Cravatt BF, Elphick MR. Localization of N-acyl phosphatidylethanolamine phospholipase d (NAPE-PLD) expression in mouse brain: a new perspective on N-acylethanolamines as neural signaling molecules. J Comp Neurol. 2008; 506:604–615. [PubMed: 18067139]

Eriksson NP, Persson JK, Svensson M, Arvidsson J, Molander C, Aldskogius H. A quantitative analysis of the microglial cell reaction in central primary sensory projection territories following peripheral nerve injury in the adult rat. Exp Brain Res. 1993; 96:9–27.

Farquhar-Smith WP, Egertová M, Bradbury EJ, McMahon SB, Rice ASC, Elphick MR. Cannabinoid CB1 receptor expression in rat spinal cord. Mol Cell Neurosci. 2000; 15:510–521. [PubMed: 10860578]

Feldblum S, Dumoulin A, Anoal M, Sandillon F, Privat A. Comparative distribution of GAD65 and GAD67 mRNAs and proteins in the rat spinal cord supports a differential regulation of these two glutamate decarboxylases in vivo. J Neurosci Res. 1995; 42:742–757. [PubMed: 8847736]

Gao Y, Vasilyev DV, Goncalves MB, Howell FV, Hobbs C, Reisenberg M, Shen R, Zhang MY, Strassle BW, Lu P, Mark L, Piesla MJ, Deng K, Kouranova EV, Ring RH, Whiteside GT, Bates B, Walsh FS, Williams G, Pangalos MN, Samad TA, Doherty P. Loss of retrograde endocannabinoid signaling and reduced adult neurogenesis in diacylglycerol lipase knock-out mice. J Neurosci. 2010; 30:2017–2024. [PubMed: 20147530]

Garrison CJ, Dougherty PM, Kajander KC, Carlton SM. Staining of glial fibrillary acidic protein (GFAP) in lumbar spinal cord increases following a sciatic nerve constriction injury. Brain Res. 1991; 565:1–7. [PubMed: 1723019]

Graeber MB. Changing face of microglia. Science. 2010; 330:783–788. [PubMed: 21051630]

Guo A, Vulchanova L, Wang J, Li X, Elde R. Immunocytochemical localization of the vanilloid receptor 1 (VR1): relationship to neuropeptides, the P2X3 purinoceptor abd IB4 binding sites. Eur J Neurosci. 1999; 11:946–958. [PubMed: 10103088]

Haydon PG, Carmingnoto G. Astrocyte control of synaptic transmission and neurovascular coupling. Physiol Rev. 2006; 86:1009–1031. [PubMed: 16816144]

Hegyi Z, Kis G, Holló K, Leden C, Antal M. Neuronal and glial localization of the cannabinoid-1 receptor in the superficial spinal dorsal horn of the rodent spinal cord. Eur J Neurosci. 2009; 30:251–262. [PubMed: 19614976]

Herkenham M, Lynn AB, Johnson MR, Melvin LS, de Costa BR, Rice KC. Characterization and localization of cannabinoid receptors in rat brain: a quantitative in vitro autoradiographic study. J Neurosci. 1991; 11:563–583. [PubMed: 1992016]

Herzberg U, Eliav E, Bennett GJ, Kopin IJ. The analgesic effects of R(+)-WIN 55,212–2 mesylate, a high affinity cannabinoid agonist, in a rat model of neuropathic pain. Neurosci Lett. 1997; 221:157–60. [PubMed: 9121688]

Hohmann AG, Martin WJ, Tsou K, Walker JM. Inhibition of noxious stimulus-evoked activity of spinal cord dorsal horn neurons by the cannabinoid WIN55,212–2. Life Sci. 1995; 56:2111–2118. [PubMed: 7776839]

Hohmann AG, Tsou K, Walker JM. Cannabinoid modulation of wide dynamic range neurons in the lumbar dorsal horn of the rat by spinally administered WIN55,212–2. Neurosci Lett. 1998; 257:119–122. [PubMed: 9870334]

Hohmann AG, Tsou K, Walker JM. Cannabinoid suppression of noxious heat-evoked activity in wide dynamic range neurons in the lumbar dorsal horn of the rat. J Neurophysiol. 1999; 81:575–583. [PubMed: 10036261]

Kano M, Ohno-Shosaku T, Hashimotodani Y, Uchigashima M, Watanabe M. Endocannabinoid-mediated control of synaptic transmission. Physiol Rev. 2009; 89:309–380. [PubMed: 19126760]

Katona I, Freund TF. Endocannabinoid signaling as a synaptic circuit breaker in neurological disease. Nat Med. 2008; 14:923–930. [PubMed: 18776886]

Katona I, Sperlágh B, Sík A, Kőfalvi A, Vizi ES, Mackie K, Freund TF. Presynaptically located CB1 cannabinoid receptors regulate GABA release from axon terminals of specific hippocampal interneurons. J Neurosci. 1999; 19:4544–4558. [PubMed: 10341254]

Katona I, Urbán GM, Wallace M, Ledent C, Jung KM, Piomelli D, Mackie K, Freund TF. Molecular composition of the endocannabinoid system at glutamatergic synapses. J Neurosci. 2006; 26:5628–5637. [PubMed: 16723519]

Kawamura Y, Fukaya M, Maejima T, Yoshida T, Miura E, Watanabe M, Ohno-Shosaku T, Kano M. The CB1 cannabinoid receptor is the major cannabinoid receptor at excitatory presynaptic sites in the hippocampus and cerebellum. J Neurosci. 2006; 26:2991–3001. [PubMed: 16540577]

Kelly S, Chapman V. Selective cannabinoid CB1 receptor activation inhibits spinal nociceptive transmission in vivo. J Neurophysiol. 2001; 86:3061–3064. [PubMed: 11731561]

Kim J, Alger BE. Inhibition of cyclooxygenase-2 potentiates retrograde endocannabinoid effects in hippocampus. Nat Neurosci. 2004; 7:697–698. [PubMed: 15184902]

Kim J, Alger BE. Reduction in endocannabinoid tone is a homeostatic mechanism for specific inhibitory synapses. Nature Neurosci. 2010; 13:592–600. [PubMed: 20348918]

Kreitzer AC, Regehr WG. Retrograde inhibition of presynaptic calcium influx by endogenous cannabinoids at excitatory synapses onto Purkinje cells. Neuron. 2001; 29:717–727. [PubMed: 11301030]

Kreitzer AC, Carter AG, Regehr WG. Inhibition of interneuron firing extends the spread of endocannabinoid signaling in the cerebellum. Neuron. 2002; 34:787–796. [PubMed: 12062024]

Laemmli UK. Cleavage of structural proteins during the assembly of the head of bacteriophage T4. Nature. 1970; 227:680–685. [PubMed: 5432063]

La Rana G, Russo R, Campolongo P, Bortolato M, Mangieri RA, Cuomo V, Iacono A, Raso GM, Meli R, Piomelli D, Calignano A. Modulation of neuropathic and inflammatory pain by the endocannabinoid transport inhibitor AM404 [N-(4-hydroxyphenyl)-eicosa-5,8,11,14-tetraenamide]. J Pharmacol Exp Ther. 2006; 317:1365–1371. [PubMed: 16510698]

Leung D, Saghatelian A, Simon GM, Cravatt BF. Inactivation of N-acyl phosphatidylethanolamine phospholipase D reveals multiple mechanisms for the biosynthesis of endocannabinoids. Biochemistry. 2006; 45:4720–4726. [PubMed: 16605240]

Li JL, Fujimaya F, Kaneko T, Mizuno N. Expression of vesicular glutamate transporters, VGluT1 and VGluT2, in axon terminals of nociceptive primary afferent fibers in the superficial layers of the medullary and spinal dorsal horns of the rat. J Comp Neurol. 2003; 457:236–249. [PubMed: 12541308]

Liu J, Wang L, Harvey-White J, Osei-Hyiaman D, Razdan R, Gong Q, Chan AC, Zhou Z, Huang BX, Kim HY, Kunos G. A biosynthetic pathway for anadamide. Proc Natl Acad Sci USA. 2006; 103:13345–13350. [PubMed: 16938887]

Liu J, Wang L, Harvey-White J, Huang BX, Kim HY, Luquet S, Palmiter RD, Krystal G, Rai R, Mahadevan A, Razdan RK, Kunos G. Multiple pathways involved in the biosynthesis of anandamide. Neuropharmacol. 2008; 54:1–7.

Liu CH, Heynen AJ, Shuler MG, Bear MF. Cannabinoid receptor blockade reveals parallel plasticity mechanisms in different layers of mouse visual cortex. Neuron. 2008; 58:340–345. [PubMed: 18466745]

Ludányi A, Hu SSJ, Yamazaki M, Tanimura A, Piomelli D, Watanabe M, Kano M, Sakimura K, Maglóczky Z, Mackie K, Freund TF, Katona I. Complementary synaptic distribution of enzymes responsible for synthesis and inactivation of the endocannabinoid 2-arachidonoylglycerol in the human hippocampus. Neuroscience. 2011; 174:50–63. [PubMed: 21035522]

Mackie M, Hughes DI, Maxwell DJ, Tillakaratne NJK, Todd AJ. Distribution and co-localization of glutamate decarboxylase isoforms in the rat spinal cord. Neuroscience. 2003; 119:461–472. [PubMed: 12770560]

Marinelli S, Pacioni S, Bisogno T, Di Marzo V, Prince DA, Hugunard JR, Bacci A. The endocannabinoid 2-arachidonoylglycerol is responsible for the slow self-inhibition in neocortical interneurons. J Neurosci. 2008; 28:13532–13541. [PubMed: 19074027]

Marsicano G, Goodenough S, Monory K, Hermann H, Eder M, Cannich A, Azad SC, Grazia Casio M, Ortega Gutiérrez S, Van der Stelt M, López-Rodriguez ML, Casanova E, Schütz G, Zieglgänsberger W, Di Marzo V, Behl C, Lutz B. CB1 cannabinoid receptors and on-demand defense against excitotoxicity. Science. 2003; 302:84–88. [PubMed: 14526074]

Martin DL, Liu H, Martin SB, Wu SJ. Structural features and regulatory properties of the brain glutamate decarboxylases. Neurochem Int. 2000; 37:111–119. [PubMed: 10812196]

Matsuda LA, Bonner TI, Lolait SJ. Localization of cannabinoid receptor mRNA in rat brain. J Comp Neurol. 1993; 327:535–550. [PubMed: 8440779]

Matsuda LA, Lolait SJ, Brownstein MJ, Young AC, Bonner TI. Structure of a cannabinoid receptor and functional expression of the cloned cDNA. Nature. 1990; 346:561–564. [PubMed: 2165569]

McClung JR, Castro AJ. Rexed's laminar scheme as it applies to the rat cervical spinal cord. Exp Neurol. 1978; 58:145–148. [PubMed: 618738]

McNeill DL, Chung K, Hulsebosch CE, Bolender RP, Coggeshall RE. Numbers of synapses in laminae I–IV of the rat dorsal horn. J Comp Neurol. 1988; 278:453–460. [PubMed: 3216052]

Mechoulam R, Ben-Shabat S, Hanus L, Ligunsky M, Kaminski NE, Schatz AR, Gopher A, Almog S, Martin BR, Compton DR. Identification of an endogenous 2-monoglyceride, present in canine gut, that binds to cannabinoid receptors. Biochem Pharmacol. 1995; 50:83–90. [PubMed: 7605349]

Molander C, Hongpaisan J, Evensson M, Aldskogius H. Glial cell reactions in the spinal cord after sensory nerve stimulation are associated with axonal injury. Brain Res. 1997; 747:122–129. [PubMed: 9042535]

Molander C, Xu Q, Grant G. The cytoarchitectonic organization of the spinal cord in the rat. I. The lower thoracic and lumbosacral cord. J Comp Neurol. 1984; 230:133–141. [PubMed: 6512014]

Morishita W, Marie H, Malenka RC. Distinct triggering and expression mechanisms underlie LTD of AMPA and NMDA synaptic responses. Nat Neurosci. 2005; 8:1043–50. [PubMed: 16025109]

Morisset V, Urban L. Cannabinoid-induced presynaptic inhibition of glutamatergic EPSCs in substantia gelatinosa neurons of the rat spinal cord. J Neurophysiol. 2001; 86:40–48. [PubMed: 11431486]

Nagy B, Fedonidis C, Photiou A, Wahba J, Paule CC, Ma D, Buluwela L, Nagy I. Capsaicin-sensitive primary sensory neurons in the mouse express N-acyl phosphatidylethanolamine phospholipase D. Neuroscience. 2009; 161:572–577. [PubMed: 19327387]

Nasu F. Analysis of calcitonin gene-related peptide (CGRP)-containing nerve fibres in the rat spinal cord using light and electron microscopy. J Electron Microsc. 1999; 48:267–275.

Navarrate M, Araque A. Endocannabinoids mediate neuron-astrocyte communication. Neuron. 2008; 57:883–893. [PubMed: 18367089]

Nedergaard M, Ransom B, Goldman SA. New roles for astrocytes: Redefining the functional architecture of the brain. Trends Neurosci. 2003; 26:523–530. [PubMed: 14522144]

Nyilas R, Dudok B, Urbán GM, Mackie K, Watanabe M, Cravatt BF, Freund TF, Katona I. Enzymatic machinery for endocannabinoid biosynthesis associated with calcium stores in glutamatergic axon terminals. J Neurosci. 2008; 28:1058–1063. [PubMed: 18234884]

Nyilas R, Gregg LC, Mackie K, Watanabe M, Zimmer A, Hohmann AG, Katona I. Molecular architecture of endocannabinoid signaling at nociceptive synapses mediating analgesia. Eur J Neurosci. 2009; 29:1964–1978. [PubMed: 19453631]

Ohno-Shosaku T, Maejima T, Kano M. Endogenous cannabinoids mediate retrograde signals from depolarized postsynaptic neurons to presynaptic terminals. Neuron. 2001; 29:729–738. [PubMed: 11301031]

Okamoto Y, Morishita J, Tsuboi K, Tonai T, Ueda N. Molecular characterization of a phospholipase D generating anandamide and its congeners. J Biol Chem. 2004; 279:5298–5305. [PubMed: 14634025]

Okamoto Y, Wang J, Morishita J, Ueda N. Biosynthetic pathways of the endocannabinoid anandamide. Chem Biodivers. 2007; 4:1842–1857. [PubMed: 17712822]

Oliveira ALR, Hydling F, Olsson E, Shi T, Edwards RH, Fujiyama F, Kaneko T, Hökfelt T, Cullheim S, Meister B. Cellular localization of three vesicular glutamate transporter mRNAs and proteins in rat spinal cord and dorsal root ganglia. Synapse. 2003; 50:117–129. [PubMed: 12923814]

Pacher P, Batkai S, Kunos G. The endocannabinoid system as an emerging target of pharmacotherapy. Pharmacol Rev. 2006; 58:389–462. [PubMed: 16968947]

Pernia-Andrade AJ, Kato A, Witschi R, Nyilas R, Katona I, Freund TF, Watanabe M, Filitz J, Koppert W, Schüttler J, Ji G, Neugebauer V, Marsicano G, Lutz B, Vanegas H, Zeilhofer HU. Spinal endocannabinoids and CB1 receptors mediate C-fiber-induced heterosynaptic pain sensitization. Science. 2009; 325:760–764. [PubMed: 19661434]

Piomelli D. The molecular logic of endocannabinoid signalling. Nat Rev Neurosci. 2003; 4:873–884. [PubMed: 14595399]

Ribeiro da Silva, A.; De Korninck, Y. Morphological and neurochemical organization of the spinal dorsal horn. In: Basbaum, AI.; Bushnell, MC., editors. Science of pain. Oxford: Elsevier; 2009. p. 279-310.

Rodriquez JJ, Mackie K, Pickel VM. Ultrastructural localization of the CB1 cannabinoid receptor in mu-opioid receptor patches of the rat caudate putamen nucleus. J Neurosci. 2001; 21:823–833. [PubMed: 11157068]

Runyan SA, Roy RR, Zhong H, Phelps PE. L1 cell adhesion molecule is not required for small-diameter primary afferent sprouting after deafferentation. Neuroscience. 2007; 150:959–969. [PubMed: 18022323]

Salio C, Doly S, Fischer J, Franzoni MF, Conrath M. Neuronal and astrocytic localization of the cannabinoid receptor-1 in the dorsal horn of the rat spinal cord. Neurosci Lett. 2002; 329:13–16. [PubMed: 12161251]

Schmid HHO, Schmid PC, Berdyshev EV. Cell signaling by endocannabinoids and their congeners: Questions of selectivity and other challenges. Chem Phys Lipids. 2002; 121:111–134. [PubMed: 12505695]

Scholz J, Woolf CJ. the neuropathic pain triad: neurons, immune cells and glia. Nat Neurosci. 2007; 11:1361–1368. [PubMed: 17965656]

Simon GM, Cravatt BF. Endocannabinoid biosynthesis proceeding through glycerophospho-N-acyl ethanolamine and a role for alpha/beta-hydrolase 4 in this pathway. J Biol Chem. 2006; 281:26465–26472. [PubMed: 16818490]

Simon GM, Cravatt BF. Anandamide biosynthesis catalyzed by the phosphodiesterase GDE1 and detection of glycerophospho-N-acyl ethanolamine precursors in mouse brain. J Biol Chem. 2008; 283:9341–9349. [PubMed: 18227059]

Soghomonian JJ, Martin DL. Two isoforms of glutamate decarboxylase: why? Trend Pharmacol Sci. 1988; 19:500–505.

Stella N, Piomelli D. Receptor-dependent formation of endogenous cannabinoids in cortical neurons. Eur J Pharmacol. 2001; 425:189–196. [PubMed: 11513837]

Stella N, Schweitzer P, Piomelli D. A second endogenous cannabinoid that modulates long-term potentiation. Nature. 1997; 388:773–778. [PubMed: 9285589]

Streit WJ. An improved staining method for rat microglial cells using the lectin from Griffonia simplicifolia (GSA I-B4). J Histochem Cytochem. 1990; 38:1683–1686. [PubMed: 2212623]

Suarez J, Bermúdez-Silva FJ, Mackie K, Ledent C, Zimmer A, Cravatt BF, De Fonseca FR. Immunohistochemical description of the endogenous cannabinoid system in the rat cerebellum and functionally related nuclei. J Comp Neurol. 2008; 509:400–421. [PubMed: 18521853]

Sugiura T, Kobayashi Y, Oka S, Waku K. Biosynthesis and degradation of anandamide and 2-arachidonoylglycerol and their possible physiological significance. Prostaglandins Leukot Essent Fatty Acids. 2002; 66:173–092. [PubMed: 12052034]

Sugiura T, Kondo S, Sukagawa A, Nakane S, Shinoda A, Itoh K, Yamashita A, Waku K. 2-Arachidonoylglycerol: a possible endogenous cannabinoid receptor ligand in brain. Biochem Biophys Res Commun. 1995; 215:89–97. [PubMed: 7575630]

Sugiura T, Kondo S, Sukagawa A, Tonegawa T, Nakane S, Yamashita A, Waku K. N-arachidonoylethanolamine (anandamide), an endogenous cannabinoid receptor ligand, and related lipid molecules in the nervous tissues. J Lipid Mediat Cell Signal. 1996; 14:51–6. [PubMed: 8906545]

Suter MR, Wen YR, Decosterd I, Ji RR. Do glial cells control pain? Neuron Glia Biol. 2007; 3:255–268. [PubMed: 18504511]

Tanimura A, Yamazaki M, Hashimotodani Y, Ushigashima M, Kawata S, Abe M, Kita Y, Hashimoto K, Shimizu T, Watanabe M, Sakimura K, Kano M. The endocannabinoid 2-arachidonoylglycerol produced by diacylglycerol lipase α mediates retrograde suppression of synaptic transmission. Neuron. 2010; 65:320–327. [PubMed: 20159446]

Todd AJ, Hughes DI, Polgár E, Nagy GG, Mackie M, Ottersen OP, Maxwell DJ. The expression of vesicular glutamate transporters VGLUT1 and VGLUT2 in neurochemically defined axonal populations in the rat spinal cord with emphasis on the dorsal horn. Eur J Neurosci. 2003; 17:13–27. [PubMed: 12534965]

Tran TS, Alijani A, Phelps PE. Unique developmental patterns of GABAergic neurons in rat spinal cord. J Comp Neurol. 2003; 456:112–126. [PubMed: 12509869]

Traub RJ, Solodkin A, Ruda MA. Calcitonin gene-related peptide immunoreactivity in the cat lumbosacral spinal cord and the effects of multiple dorsal rhizotomies. J Comp Neurol. 1989; 287:225–237. [PubMed: 2794127]

Tsou K, Brown S, Sanudo-Pena MC, Mackie K, Walker JM. Immunohistochemical distribution of cannabinoid CB1 receptors in the rat central nervous system. Neuroscience. 1998; 83:393–411. [PubMed: 9460749]

van der Stelt M, Trevisani M, Vellani V, De Petrocellis L, Moriello AS, Campi B, McNaughton P, Geppetti P, Di Marzo V. Anandamide acts as an intracellular messenger amplifying Ca^{2+} influx via TRPV1 channels. EMBO J. 2005; 24:3026–3037. [PubMed: 16107881]

Villeda SA, Akopians AL, Babayan AH, Basbaum AI, Phelps PE. Absence of reelin results in altered nociception and aberrant neuronal positioning in the dorsal spinal cord. Neuroscience. 2006; 139:1385–1396. [PubMed: 16580148]

Volterra, A.; Bezzi, P. The tripartite synapse: Glia. In: Volterra, A.; Magistretti, PJ.; Haydon, PG., editors. Synaptic transmission. New York: Oxford UP; 2002. p. 164-168.

Walter L, Stella L. Endothelin-1 increases 2-arachidonyl glycerol (2-AG) production in astrocytes. Glia. 2003; 44:85–90. [PubMed: 12951660]

Walter L, Stella N. Cannabinoids and neuroinflammation. Br J Pharmacol. 2004; 141:775–85. [PubMed: 14757702]

Walter L, Dinh T, Stella N. ATP induces a rapid and pronounced increase in 2-arachidonoylglycerol production by astrocytes, a response limited by monoacylglycerol lipase. J Neurosci. 2004; 24:8068–74. [PubMed: 15371507]

Walter L, Franklin A, Witting A, Möller T, Stella N. Astrocytes in culture produce anadamide and other acylethanolamides. J Biol Chem. 2002; 277:20869–20876. [PubMed: 11916961]

Walter L, Franklin A, Witting A, Wade C, Xie Y, Kunos G, Mackie K, Stella N. Non-psychotic cannabinoid receptors regulate microglial cell migration. J Neurosci. 2003; 23:1398–1405. [PubMed: 12598628]

Wang Z, Kai L, Day M, Ronesi J, Yin HH, Ding J, Tkatch T, Lovinger DM, Surmeier DJ. Dopaminergic control of corticostriatal long-term synaptic depression in medium spiny neurons is mediated by cholinergic interneurons. Neuron. 2006; 50:443–452. [PubMed: 16675398]

Willis, WD.; Coggeshall, RE. Primary afferent neurons and the spinal dorsal horn. Vol. 1. New York: Kluwer Academic/Plenum Publishers; 2004. Sensory mechanisms of the spinal cord.

Wilson RI, Nicoll RA. Endogenous cannabinoids mediate retrograde signalling at hippocampal synapses. Nature. 2001; 410:588–592. [PubMed: 11279497]

Wilson RI, Nicoll RA. Endocannabinoid signaling in the brain. Science. 2002; 296:678–82. [PubMed: 11976437]

Witting A, Walter L, Wacker J, Moller T, Stella N. $P2X_7$ receptors control 2-arachidonoylglycerol production by microglial cells. Proc Natl Acad Sci USA. 2004; 101:3214–3219. [PubMed: 14976257]

Wang J, Ueda N. Biology of endocannabinoid synthetic system. Prostaglandins Lipid Med. 2009; 89:112–119.

Yoshida T, Fukaya M, Uchigashima M, Miura E, Kamiya H, Kano M, Watanabe M. Localization of diacylglycerol lipase-α around postsynaptic spine suggests close proximity between production site of an endocannabinoid, 2-arachidonoyl-glycerol, and presynaptic cannabinoid CB1 receptor. J Neurosci. 2006; 22:1690–1697. [PubMed: 11880498]

Zhang F, Vadakkan KI, Kim SS, Wu LJ, Shang Y, Zhuo M. Selective activation of microglia in spinal cord but not higher cortical regions following nerve injury in adult mouse. Mol Pain. 2008; 4:1–16. [PubMed: 18171466]

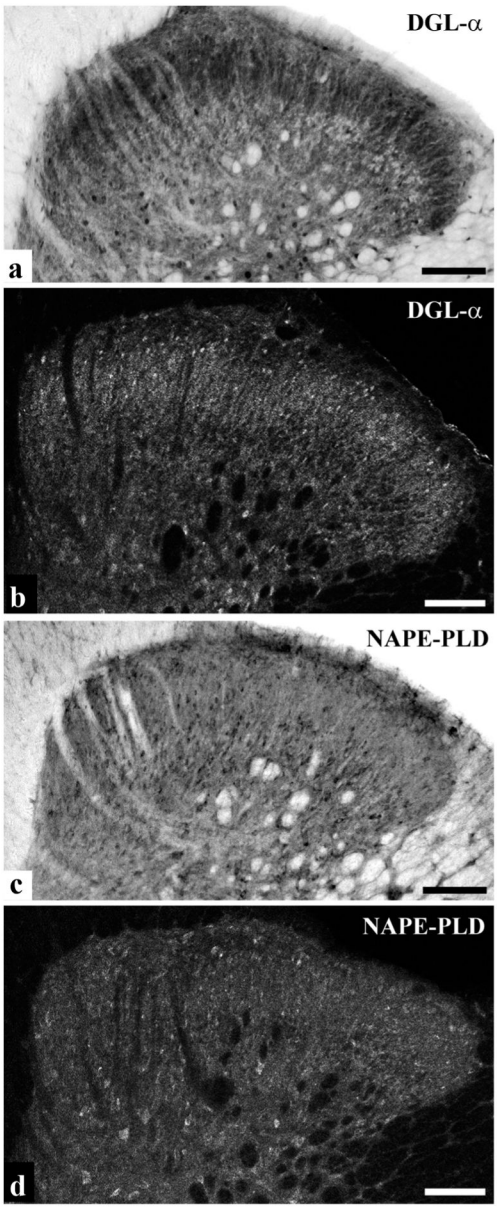

Figure 1.

The distribution of DGLα and NAPE-PLD immunoreactivity in the spinal dorsal horn. a and b, Photomicrograph showing immunoreactivity for DGLα in the spinal dorsal horn of rats following immunoperoxidase (a) and immunofluorescence (b) staining. We observed an abundant punctuate immunoreactivity for DGLα. Lamina II of the superficial spinal dorsal horn appeared as a heavily stained band, whereas lamina I was more sparsely stained. Besides the characteristic punctuate labeling, larger immunoreactive spots resembling somata of neurons or glial cells were also scattered throughout both the gray and white matters. c and d, Photomicrograph showing immunoreactivity for NAPE-PLD in the dorsal horn of rat's spinal cord following immunoperoxidase (c) and immunofluorescence (d) staining. Generally, we observed a homogeneous punctuate immunostaining for NAPE-PLD, but larger NAPE-PLD immunoreactive spots resembling somata of neurons or glial cells were also seen both in the gray and white matter. Note that the immunoperoxidase and

immunofluorescent stainings show very similar patterns of immunoreactivity. Scale bar: 100 μm.

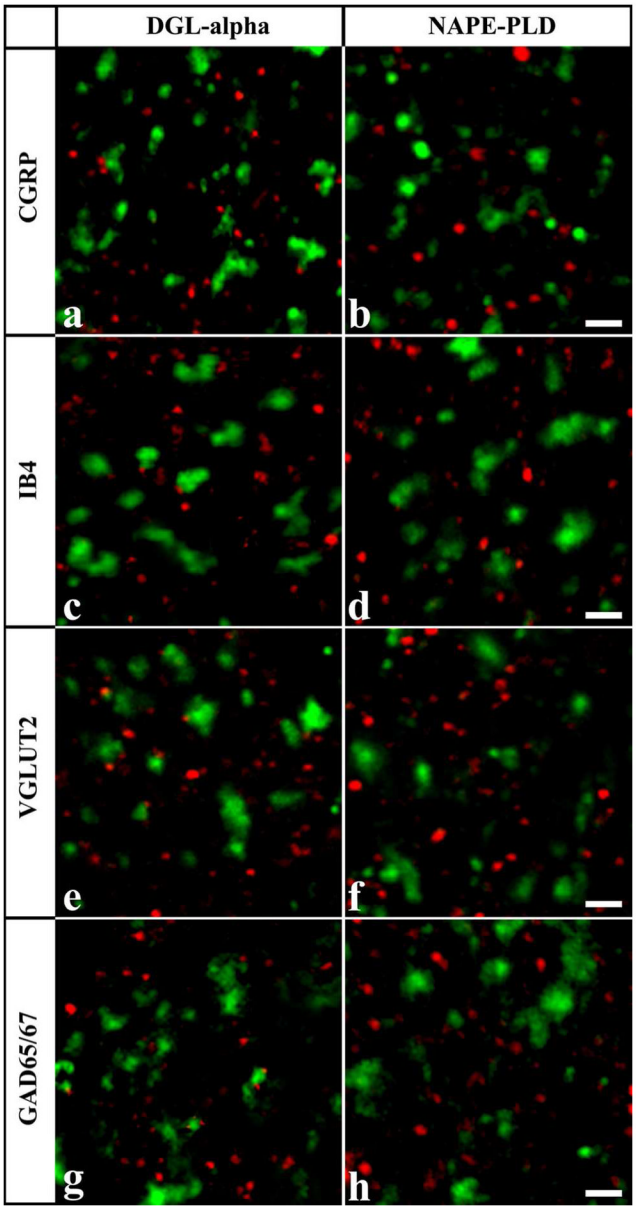

Figure 2.

Co-localization of DGLα and NAPE-PLD with axonal markers. Micrographs of single 1μm thick laser scanning confocal optical sections assessing co-localization between immunolabeling for DGLα (red; a, c, e, g) or NAPE-PLD (red; b, d, f, h) and immunoreactivity for markers that are specific for axon terminals of specific populations of peptidergic (CGRP, green; a, b) and non-peptidergic (IB4-binding, green; c, d) nociceptive primary afferents, as well as for axon terminals of putative excitatory (VGLUT2, green; e, f) and inhibitory (GAD65/67, green; g, h) intrinsic neurons in the superficial spinal dorsal horn. Note that mixed colors (yellow) that may indicate double labeled structures are not observed on the superimposed images. Scale bar: 2 μm.

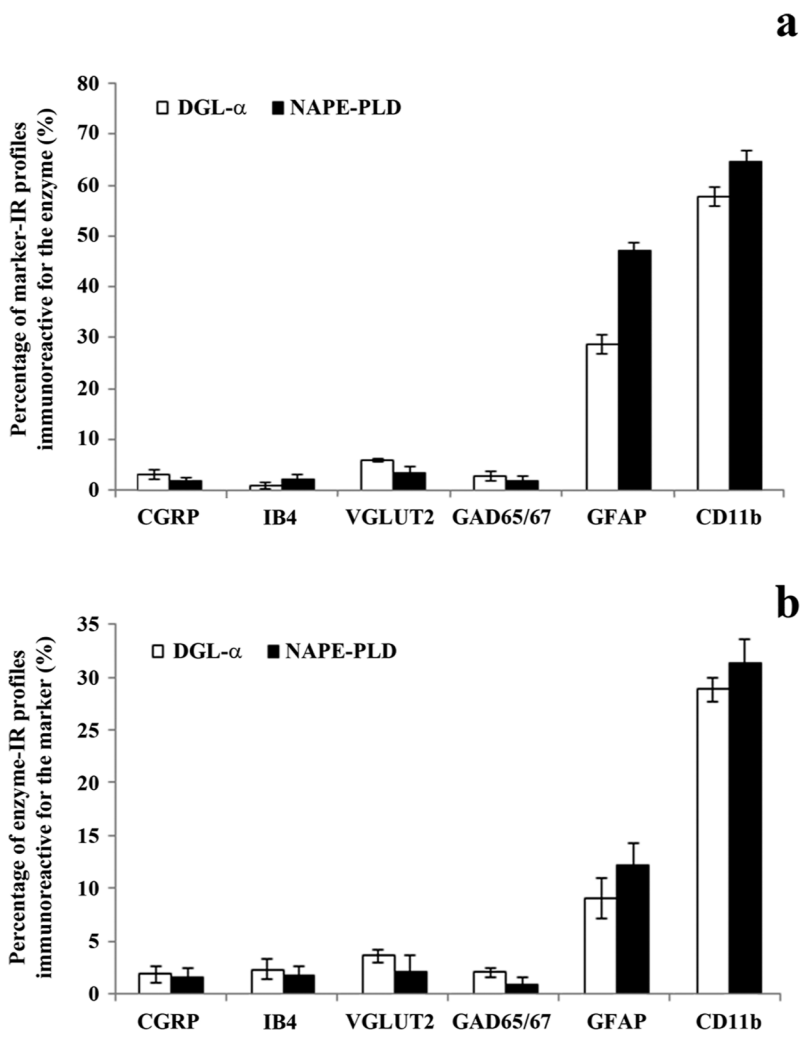

Figure 3.

The degree of co-localization of DGLα and NAPE-PLD with axonal and glial markers. Histograms showing the degree of co-localization between immunoreactivity for DGLα or NAPE-PLD and selected axonal and glial markers in laminae I–II of the spinal dorsal horn. a) Percentage of profiles immunoreactive for the applied axonal and glial markers that were found to be labeled also for DGLα or NAPE-PLD. b) Percentage of profiles immunoreactive for DGLα or NAPE-PLD that were found to be labeled also for the applied axonal and glial markers. Data are shown as mean ± SEM.

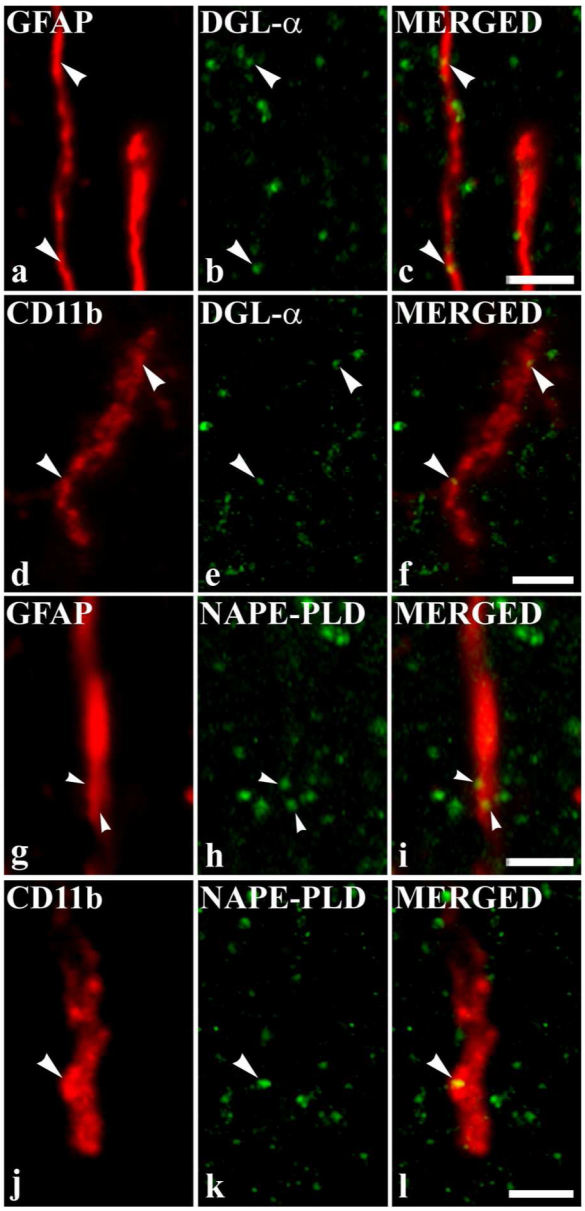

Figure 4.

Co-localization of DGLα and NAPE-PLD with glial markers. Micrographs of single 1.6 μm thick laser scanning confocal optical section (compressed images of three consecutive 1 μm thick optical sections with 0.3 μm separation in the Z axis) illustrating the co-localization between immunolabeling for DGLα (green; b) and immunoreactivity for a marker which is specific for astrocytes (GFAP, red; a); between immunolabeling for DGLα (green; e) and immunoreactivity for a marker which is specific for microglial cells (CD11b, red; d); between immunolabeling for NAPE-PLD (green; h) and immunoreactivity for a marker which is specific for astrocytes (GFAP, red; g); between immunolabeling for NAPE-PLD (green; k) and immunoreactivity for a marker which is specific for microglial cells (CD11b, red; j) in the superficial spinal dorsal horn. Mixed colors (yellow) on the superimposed image (c, f, i, l) indicate double labeled spots within the illustrated glial processes. Puncta immunoreactive for DGLα or NAPE-PLD which are also stained for the glial marker are marked with arrowheads. Scale bar: 2 μm.

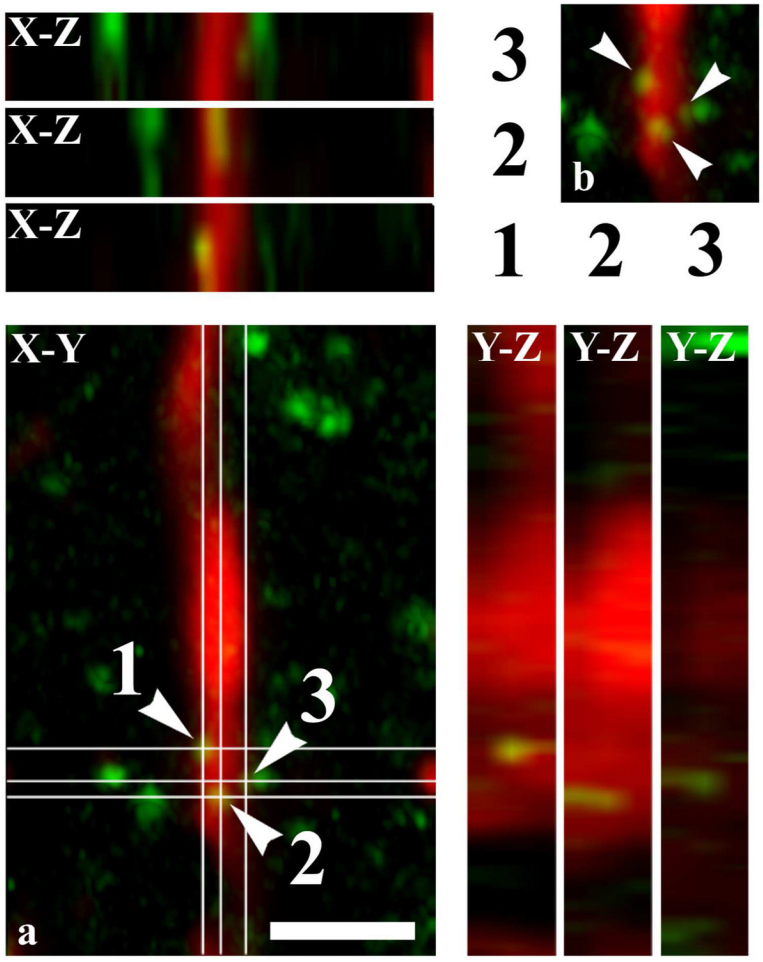

Figure 5.

Co-localization between NAPE-PLD and GFAP illustrated in X-Y, X-Z and Y-Z projections of confocal optical sections. Micrographs of a singe1.6 μm thick laser scanning confocal optical section, shown also in Figure 6i, illustrating X-Y, X-Z and Y-Z projections of the optical section double immunostained for GFAP (red) and NAPE-PLD (green). The points of co-localization between the two markers are at the crossing point of two lines indicating the planes through which orthogonal views of X-Z and Y-Z projections were drawn. The X-Z and Y-Z images of puncta 1, 2, 3 on insert a are identified by the serial numbers of the puncta beside and above the X-Z and Y-Z projections, respectively. Insert b shows a part of insert a (without the lines indicating the planes of the orthogonal views) at the site of the NAPE-PLD immunoreactive puncta. According to the orthogonal images, as it is indicated by the mixed color (yellow), NAPE-PLD immunostained puncta 1 and 2 are within the confines of the GFAP immunoreactive profile (see the mixed color (yellow) on all the three projections). However, in case of immunoreactive punctum 3, although there appears to be some overlap between the two markers indicated by the mixed color (yellow) on the X-Y and X-Z projections, the green color on the Y-Z projectional image clearly shows that the NAPE-PLD immunoreactive punctum is not within but adjacent to the GFAP immunoreactive profile.

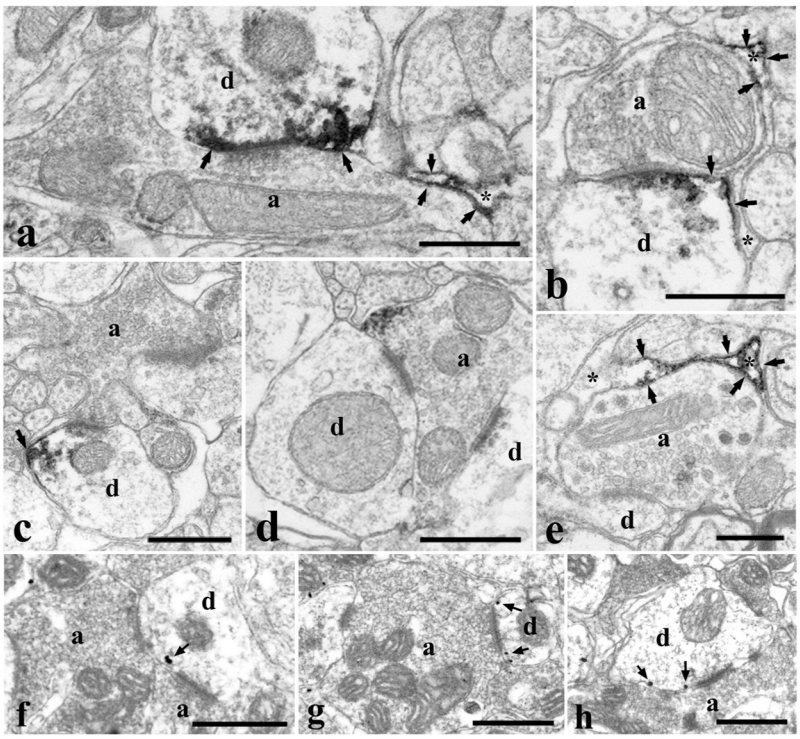

Figure 6.

Ultrastructural localization of DGLα immunoreactivity in neurons and glial cells. Electron micrographs of preembedding immunoperoxidase (a–e) and nanogold (f–h) stained sections showing the distribution of DGLα on postsynaptic dendrites (a–c, f–h) establishing synaptic contacts with axon terminals, in an axon terminal (d) and in glial profiles (a, b, e) in laminae I–II of the spinal dorsal horn. Immunoprecipitates and silver particles labeling DGLα in dendrites and axon terminal aligned along the perisynaptic surface membrane. Immunoprecipitates labeling DGLα in glial cells are also aligned along the surface membrane of glial processes. In some glial processes, the immunolabeled membrane compartments are in close vicinity to synapses (a, b). a: axon terminal, d: postsynaptic dendrite, asterisk: glial profile. Arrows point at immunoperoxidase deposits and silver intensified nanogold particles. Bars: 0.5 μm.

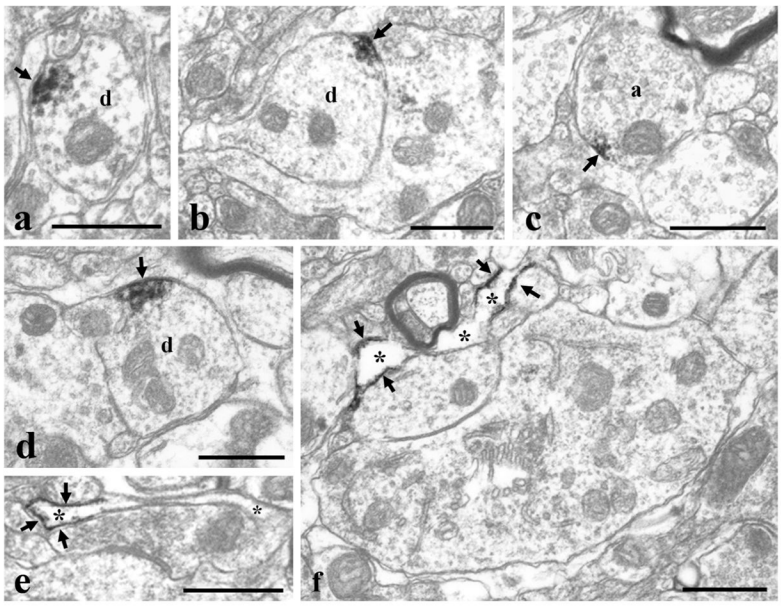

Figure 7.

Ultrastructural localization of NAPE-PLD immunoreactivity in neurons and glial cells. Electron micrographs of preembedding immunoperoxidase stained sections showing the distribution of NAPE-PLD on dendrites (a, b, d), in an axon terminal (c) and in glial profiles (e, f) in laminae I–II of the spinal dorsal horn. Immunoprecipitates labeling NAPE-PLD in dendrites, axon terminal and glial processes are aligned along the surface membrane. a: axon terminal immunoreactive for NAPE-PLD, d: postsynaptic dendrite, asterisk: glial profile. Arrows point at immunoperoxidase deposits. Bars: 0.5 μm.